Proceedings of the 29th Annual International
Conference of the IEEE EMBS
Cité Internationale, Lyon, France
August 23-26, 2007.

Powered Ankle-Foot Prosthesis for the Improvement of Amputee Ambulation

Samuel K. Au, Hugh Herr, Jeff Weber, and Ernesto C. Martinez-Villalpando

***Abstract*—This paper presents the mechanical design, control scheme, and clinical evaluation of a novel, motorized ankle-foot prosthesis, called MIT Powered Ankle-Foot Prosthesis. Unlike a conventional passive-elastic ankle-foot prosthesis, this prosthesis can provide active mechanical power during the stance period of walking. The basic architecture of the prosthesis is a unidirectional spring, configured in parallel with a force-controllable actuator with series elasticity. With this architecture, the ankle-foot prosthesis matches the size and weight of the human ankle, and is also capable of delivering high mechanical power and torque observed in normal human walking. We also propose a biomimetic control scheme that allows the prosthesis to mimic the normal human ankle behavior during walking.**

To evaluate the performance of the prosthesis, we measured the rate of oxygen consumption of three unilateral transtibial amputees walking at self-selected speeds to estimate the metabolic walking economy. We find that the powered prosthesis improves amputee metabolic economy from 7% to 20% compared to the conventional passive-elastic prostheses (Flex-Foot Ceterus and Freedom Innovations Sierra), even though the powered system is twofold heavier than the conventional devices. This result highlights the benefit of performing net positive work at the ankle joint to amputee ambulation and also suggests a new direction for further advancement of an ankle-foot prosthesis.

I. Introduction

The human ankle provides a significant amount of net positive work over the stance period of walking, especially at moderate to fast walking speeds [1]-[3]. On the contrary, commercially available ankle-foot prostheses are completely passive during stance, and consequently, they cannot provide net positive work. These prostheses typically comprise elastic bumper springs or carbon composite leaf springs that store and release energy during stance, e.g. the Flex-Foot [4]. Clinical studies indicate that transtibial amputees using these conventional passive prostheses experience many problems during locomotion, including non-symmetric gait patterns, slower self-selected walking speeds, and higher gait metabolic rates as compared to intact individuals [5][6][7]. Researchers believe [2][3][5] that the inability of conventional passive prostheses to provide net positive work over the stance period of walking is the main cause for the above clinical difficulties.

Our research goal is to develop a powered ankle-foot prosthesis[1] that is capable of providing sufficient active mechanical power or net positive work over the stance period and test if such a prosthesis can improve amputee ambulation.

A. Previous Work

Although the idea of a powered ankle-foot prosthesis has been discussed since the late 1990s, only one attempt [8] has been made to develop such a prosthesis to improve the locomotion of amputees. However, although the mechanism was built, no further publication has demonstrated its capacity to improve amputee gait compared to conventional passive-elastic prostheses. More recent work has focused on the development of quasi-passive ankle-foot prostheses [9][10][11]. Collins and Kuo [9] advanced a foot system that stores elastic energy during early stance, and then delays the release of that energy until late stance, in an attempt to reduce impact losses of the adjacent leg. Since the device does not include an actuator to actively plantar flex the ankle, no net work is performed throughout stance. Other researchers [10][11] have built prostheses that use active damping or clutch mechanisms to allow ankle angle adjustment under the gravity force or the amputee's own weight. In the commercial sector, the most advanced ankle-foot prosthesis, the Össur Proprio Foot^{TM} [12], has an electric motor to adjust the orientation of a low profile passive-elastic foot during the swing phase. Although active during the swing phase, its ankle joint is locked during stance, and therefore becomes equivalent to a passive elastic foot. Consequently, no net positive work is done at the ankle joint during stance.

B. Engineering Challenges

There are two main hurdles hindering the development of a powered ankle-foot prosthesis [5][13][14]. First, it is challenging to build an ankle-foot prosthesis that matches the size and weight of the intact ankle, but still provides a sufficiently large instantaneous power output and torque to propel an amputee. For example, the shank-ankle-foot complex of a 75 kg person weighs about 2.5 kg, while the peak power and torque at the ankle during walking can be as high as 350 W and 140 Nm, respectively [13][14]. Second, there is no clear control target or "gold standard" for the prosthesis to

This work was performed in the Biomechatronics Group at the MIT Media Lab and was supported in part by the U.S Department of Veteran's Administration under Grant V650P-3945.

S. Au is with the Department of Mechanical Engineering and the MIT Media Lab, Massachusetts Institute of Technology, Cambridge, MA, 02139 USA (corresponding author phone: 617-324-1701; e-mail: kwau@mit.edu.)

H. Herr is with the MIT Media Lab and the Harvard-MIT Division of Health Sciences and Technology, Massachusetts Institute of Technology, Cambridge, MA 02139 USA; e-mail: hherr@media.mit.edu.

J. Weber is with the MIT Media Lab, Massachusetts Institute of Technology, Cambridge, MA 02139 USA

E. Martinez-Villalpando is with the MIT Media Lab, Massachusetts Institute of Technology, Cambridge, MA 02139 USA

[1] In this paper, a powered ankle-foot prosthesis is defined as an ankle-foot prosthesis that can provide net positive work over the stance period of walking. The average net positive work done at the ankle joint at the normal self-selected walking speed (1.25 m/s) is about 0.1±0.07 J kg^{-1} [1][3].

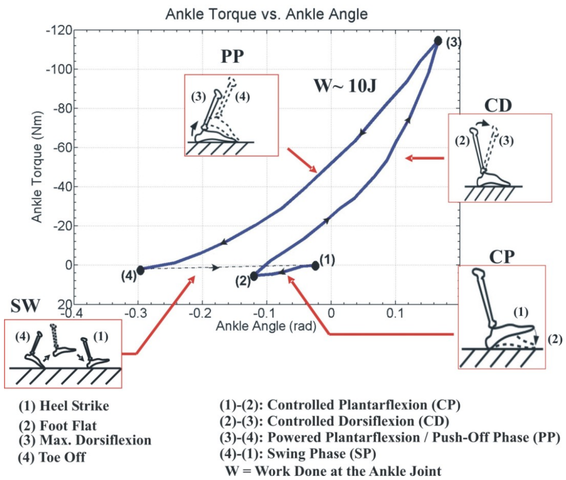

Fig. 1. A typical ankle torque-angle behaviour for a 75 kg person at his/her self-selected walking speed(1.25 m/s). Data are from [3], re-plotted in the manner of [14]. The solid line shows the ankle torque-angle behaviour during stance while the dash line shows the ankle behaviour during the swing phase.

be controlled, against which to gauge the effectiveness. It is unclear what kind of prosthetic control strategy is effective for the improvement of amputee ambulation.

C. Objectives and Outline

A key objective of this research is to address both the mechanical and control system design challenges. We design and build a novel, motorized prosthesis that fulfills the demanding human-like ankle specifications [13][14]. We also propose a finite-state controller that allows the prosthesis to mimic human ankle function during walking. Finally, we conduct clinical study to evaluate the performance of the prosthesis.

II. Design Specifications and Target Stance Phase Behavior for the Prosthesis

In this section, we review the walking biomechanics of normal human ankle and use these descriptions to define the target behavior and design specifications of the prosthesis.

A. Normal Human Ankle-Foot Walking Biomechanics

A level-ground walking gait cycle is typically defined as beginning with the heel strike of one foot and ending at the next heel strike of the same foot [15]. The main subdivisions of the gait cycle are the stance phase (60% of a gait cycle) and the swing phase (40% of a cycle). The swing phase (SW) represents the portion of the gait cycle when the foot is off the ground. The stance phase begins at heel-strike when the heel touches the floor and ends at toe-off when the same foot rises from the ground surface. From [2][3], the stance phase of walking can be divided into three sub-phases: Controlled Plantar Flexion (CP), Controlled Dorsiflexion (CD), and Powered Plantar Flexion (PP). Fig. 1 shows the typical ankle torque-angle characteristics for a 75 kg person walking at his/her self-selected speed (1.25 m/sec). The detailed descriptions for each sub-phase are provided below.

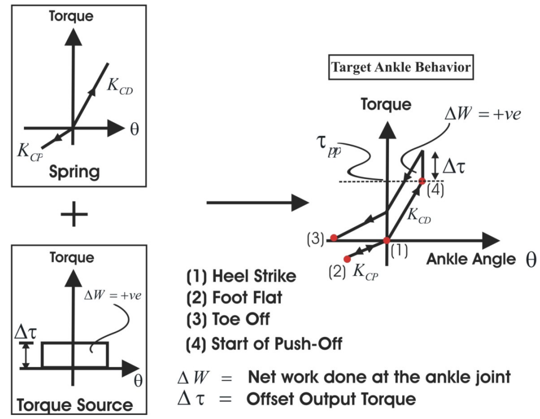

Fig. 2. Target stance phase behavior.

- CP begins at heel-strike and ends at foot-flat. During CP, the ankle behavior is consistent with a linear spring response [2][3]. The segment (1)-(2) in Fig. 1 illustrates the linear spring behavior of the ankle.
- CD begins at foot-flat and continues until the ankle reaches a state of maximum dorsiflexion. During CD, the ankle behavior can be described as a nonlinear spring for energy storage [2]. Segment (2)-(3) in Fig. 1 reveals the nonlinear spring behavior of the human ankle joint during CD.
- PP begins after CD and ends at the instant of toe-off. During PP, the ankle can be modeled as a torque source in parallel with the CD spring. The area W enclosed by the points (2), (3), and (4) shows the net work done at the ankle.
- SW begins at toe-off and ends at heel-strike. During SW, the ankle can be modeled as a position source to reset the foot to a desired equilibrium position before the next heel strike.

In summary, for level ground walking, human ankle provides three main functions: (i) it behaves as a spring with variable stiffness from CP to CD;(ii) it provides additional energy for push-off during PP; and (iii) it behaves as a position source to control the foot orientation during SW.

B. Target Stance Phase Behavior

Referring to Section I-B, the key question for the design and control is to define a target walking behavior for the prosthesis. For the swing phase, the desired behavior is just to re-position the foot to an predefined equilibrium position. For the stance phase control, instead of simply tracking ankle kinematics, it is commonly believed that the best way is to let the prosthesis mimic the "quasi-static stiffness", that is the slope of the measured ankle torque-angle curve during stance [2][3]. Mimicking the quasi-static stiffness curve of an intact ankle during walking (Fig. 1) is the main goal for the stance phase control.

A typical quasi-static stiffness curve (Fig. 1) can be decomposed into two main components: (1) a spring whose stiffness varies in a similar manner to the normal human ankle does in CP and CD. (2) a torque source that provides positive net work during late stance phase. For the ease of implementation, we modified these two components to obtain the target stance phase behavior as depicted in Fig. 2. Each component is described as follows:

1) A linear torsional spring with a stiffness that varies with the sign of the ankle angle. When the ankle angle is positive, the stiffness value will be set to K_{CD}. When the ankle angle is negative, the stiffness value will be set to K_{CP}.
2) A constant offset torque $\Delta\tau$ is used to model the torque source during PP. This offset torque is applied in addition to the torsional spring K_{CD} during PP. τ_{pp} determines the moment at which the offset torque is applied, indicated by the point (4) in Fig. 2.

It is noted that the conventional passive prostheses only provide the spring behavior but fail to supply the function of the torque source to propel the body during PP [4]. Our designed prosthesis eventually will provide both functions during stance.

C. Design specifications

Using the results from [2][3][15], the design goals for the prosthesis are summarized as follows:

- the prosthesis should be at a weight and height similar to the intact limb.
- the system must deliver a large instantaneous output power and torque during push-off.
- the system must be capable of changing its stiffness as dictated by the quasi-static stiffness of an intact ankle.
- the system must be capable of controlling joint position during the swing phase.
- the prosthesis must provide sufficient shock tolerance to prevent any damage in the mechanism during the heel-strike.

The corresponding parameters values of the above design goals are given in Table I. These parameters values are estimated based on the human data from [2][3][15][16].

TABLE I
DESIGN SPECIFICATIONS

Weight (kg)	2.5
Max. Allowable Dorsiflexion (Deg)	15
Max. Allowable Plantarflexion (Deg)	25
Peak Torque (Nm)	140
Peak Velocity (rad/s)	5.2
Peak Power (W)	350
Torque Bandwidth (Hz)	3.5
Net Work Done (J)	10J at 1.3m/s
Required Offset Stiffness (Nm/rad)	550

III. MECHANICAL DESIGN

The basic architecture of our mechanical design is a physical spring, configured in parallel to a high power output force-controllable actuator (Fig. 3). The parallel spring and the force-controllable actuator serve as the spring component and the torque source, respectively.

As can be seen in Fig. 3(c), there are five main mechanical elements in the system: a high power output d.c. motor, a transmission, a series spring, an unidirectional parallel spring, and a carbon composite leaf spring prosthetic foot. We combine the first three components to form a force-controllable actuator, called Series-Elastic Actuator(SEA). A SEA, previously developed for legged robots [17], consists of a dc motor in series with a spring (or spring structure) via a mechanical transmission. The SEA provides force control by controlling the extent to which the series spring is compressed. Using a linear potentiometer, we can obtain the force applied to the load by measuring the deflection of the series spring.

In this application, we use the SEA to modulate the joint stiffness as well as provide the constant offset torque $\Delta\tau$. As can be seen in Fig. 4, the SEA provides a stiffness value K_{CP} during CP and a stiffness value K_{CD1} from CD to PP. From points (4) to (3), it supplies both the stiffness value K_{CD1} and a constant, offset torque $\Delta\tau$.

Due to the demanding output torque and power requirements, we incorporate a physical spring, configured in parallel to the SEA, so that the load borne by the SEA is greatly reduced. Because of this fact, the SEA will have a substantially large force bandwidth to provide the active push-off during PP. To avoid hindering the foot motion during swing phase, the parallel spring is implemented as an unidirectional spring that provides an offset rotational stiffness value K_p^r only when the ankle angle is larger than zero degree (Fig. 4).

The elastic leaf spring foot is used to emulate the function of a human foot that provides shock absorption during foot strike, energy storage during the early stance period, and energy return in the late stance period. A standard prosthetic foot, Flex Foot LP Vari-Flex [12] is used in the prototype.

A. Component Selections

Broadly speaking, there are three main design decisions in this project: (1) choosing the parallel spring stiffness, (2) choosing the actuator and transmission, and (3) choosing the series spring stiffness.

1) Parallel Spring: A linear parallel spring k_p with a moment arm R_p in Fig. 3(c) provides a rotational joint stiffness K_p^r,

$$K_p^r = (k_p)(R_p)^2 \qquad (1)$$

The goal is to select the moment arm and the spring constant to provide the suggested offset stiffness in Table I. In the physical system, due to the size and weight constraints, k_p and R_p were chosen to be 770KN/m and 0.022m, respectively. Consequently, K_P^r=385rad/s. Because this value is smaller than the suggested offset stiffness(550rad/s), the SEA supplements the required joint stiffness (Fig. 4).

2) Actuator and Transmission: The goal is to select an actuator and a transmission to bracket the maximum torque and speed characteristics of the prosthesis, so as to match the intact ankle torque/power-speed requirements (Fig. 5). In our design, a 150 W d.c. brushed motor from Maxon, Inc (RE-40) was used. For the drive train system, the motor was designed

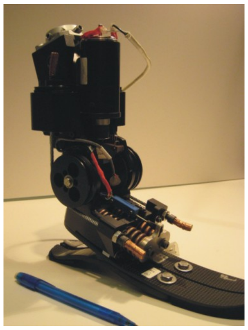

(a) Physical prototype

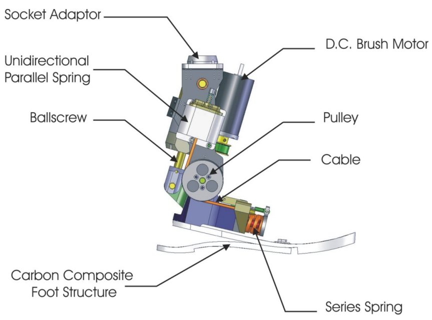

(b) CAD model

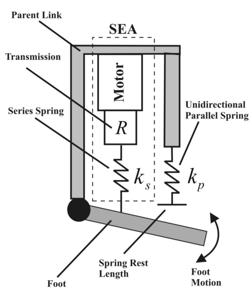

(c) Schematics

Fig. 3. Mechanical design of the prosthesis.

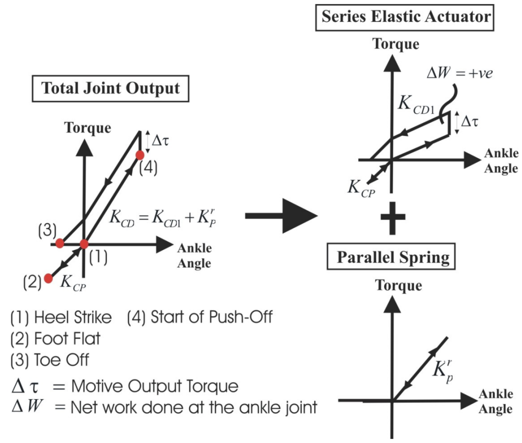

Fig. 4. Exploiting the parallel and series elasticity with an actuator.

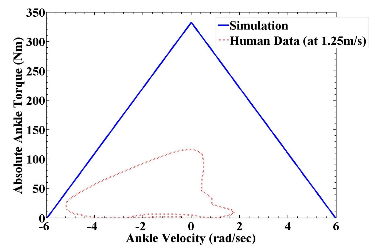

(a) Absolute Joint Torque vs. Joint Velocity

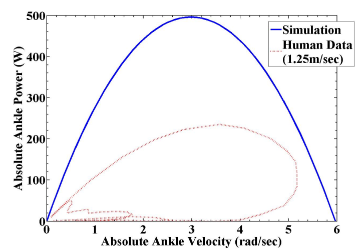

(b) Absolute Joint Power vs. Absolute Joint Velocity

Fig. 5. Comparisons of the joint torque/power-speed characteristic of the prosthesis to that of the normal human ankle during walking.

to drive a 3 mm pitch linear ballscrew via a timing-belt drive transmission with a 1.7:1 ratio. The translational movement of the ballscrew causes an angular rotation of the ankle joint via the series spring with a moment arm r=0.0375 m. The peak torque-speed characteristics of the prosthesis in Fig. 5 has shown that the prosthesis is capable of mimicking normal human ankle-foot walking behavior. Furthermore, the power output characteristic of the prosthesis was designed to match that of the intact ankle during walking.

3) Series Spring: The design goal is to have the force bandwidth of the SEA much greater than the required bandwidth specified in Table I. To this end, we conducted a bandwidth analysis for the proposed prosthesis based on a simple linear model(Fig. 6). All degrees of freedom were transferred to the translation domain of the ballscrew. M_e, B_e, and F_e represent the effective mass, damping, and linear motor force acting on effective mass, respectively, while x and k_s are the displacement and the spring constant of the series spring. Both ends of the prosthesis were fixed. The spring force F_s was considered as the system output. With the consideration of the motor saturation, the transfer function that describes the force bandwidth at large force [17] is:

$$\frac{F_s^{max}}{F_{sat}} = \frac{k_s}{M_e s^2 + (B_e + \frac{F_{sat}}{V_{sat}})s + k_s} \quad (2)$$

where F_s^{max} ,F_{sat}, and V_{sat} are the maximum output force, maximum input motor force, and maximum linear velocity of the motor respectively. They are defined as $F_{sat} = RT_{motor}^{max}$ and $V_{sat} = \frac{\omega^{max}}{R}$, where R, T_{motor}^{max}, ω^{max} are the transmission ratio, motor stall torque, and maximum motor velocity, respectively.

The bandwidth requirement can be satisfied with a series spring k_s=1200kN/m and the above transmission and motor selection. The simulation result of the large force bandwidth have shown in Fig. 7. The corresponding model parameters can be found in [16]. As can be seen, the estimated large force

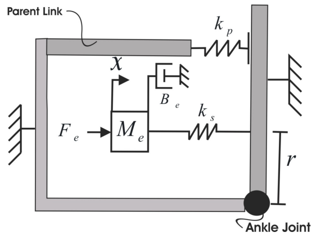

Fig. 6. A simple linear model of the prosthesis for the bandwidth analysis.

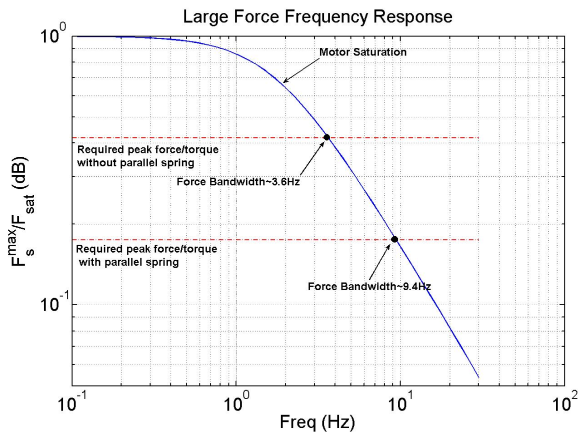

Fig. 7. Simulation result for the large force bandwidth due to motor saturation.

bandwidth of the system with and without the parallel spring was at 9.4Hz (at 50Nm) and 3.8Hz (at 120Nm), respectively. As the parallel spring shared some of the payloads of the SEA, the required peak force for the system was significantly reduced. With the parallel spring, the estimated force bandwidth were much larger than the designed one.

IV. Control System

Finite-state controllers are usually used in locomotion assistive/prosthetic devices such as A/K prostheses [18][13]because gait is repetitive between strides and, within a stride, and can be characterized into distinct finite numbers of sub-phases. The human ankle also demonstrates such kind of periodic and phasic properties during walking. This motivates the usage of a finite-state controller to control the powered prosthesis. Referring to Section II-B, the finite-state controller should be designed to replicate the target stance phase behavior. To this end, a finite-state controller for level-ground walking was implemented (Fig. 8). The details of the proposed finite-state controller for level-ground walking are discussed as follows.

A. Stance Phase Control

Three states (CP, CD, and PP) were designed for stance phase control. Descriptions for each state are shown below.

- CP begins at heel-strike and ends at mid-stance. During CP, the prosthesis outputs a joint stiffness, K_{CP}.
- CD begins at mid-stance and ends at PP or toe-off, depending on the measured total ankle torque T_{ankle}. During CD, the prosthesis outputs a joint stiffness, K_{CD}, where $K_{CD} = K_p^r + K_{CD1}$.
- PP begins only if the measured total ankle torque, T_{ankle} is larger than the predefined torque threshold, τ_{pp}. Otherwise, it remains in state CD until the foot is off the ground. During PP, the prosthesis outputs a constant offset torque, $\Delta\tau$ superimposing the joint stiffness, K_{CD} as an active push-off.

K_{CP}, K_{CD}, τ_{pp}, and $\Delta\tau$ are the main parameters affecting the ankle performance during the stance phase control. In particular, the offset torque is directly related to the amount of net work done at the ankle joint. These parameter values were chosen based on the user's walking preference during experiments. The stance phase control for a typical gait cycle is graphically depicted in Fig. 8.

B. Swing Phase Control

Another three states (SW1, SW2, and SW3) were designed for the swing phase control. Descriptions for each state are shown below.

- SW1 begins at toe-off and ends in a given time period, t_H. During SW1, the prosthesis servos the foot to a predefined foot position, θ_{toeoff} for foot clearance.
- SW2 begins right after SW1 and finishes when the foot reaches zero degree. During SW2, the prosthesis servos the foot back to the default equilibrium position $\theta_d = 0$.
- SW3 begins right after SW2 and ends at the next heel-strike. During SW3, the controller will reset the system to impedance mode and output a joint stiffness, K_{CP}.

The time period, t_H and predefined foot position, θ_{toeoff} are all tuned experimentally.

C. Sensing for State Transitions

During state transition and identification, the system mainly relied on four variables:

- Heel contact(H). H=1 indicates that the heel is on the ground, and vice versa.
- Toe contact(T). T=1 indicates that the toe is on the ground, and vice versa.
- Ankle angle (θ)
- Total ankle torque (T_{ankle})

All these triggering information can be obtained using local sensing; including foot switches to measure heel/toe contact, ankle joint encoder to measure the ankle angle, and the linear spring potentiometer to measure joint torque.

D. Low-level Servo Controllers

To support the proposed stance phase and swing phase controls, three types of low-level servo controllers were developed: (i) a high performance torque controller to provide an offset torque during push-off as well as facilitate the stiffness modulation; (ii) an impedance controller to modulate the joint stiffness during the entire stance phase; (iii) a position controller to control the foot position during the swing phase. The details of the controller designs can be found in [16].

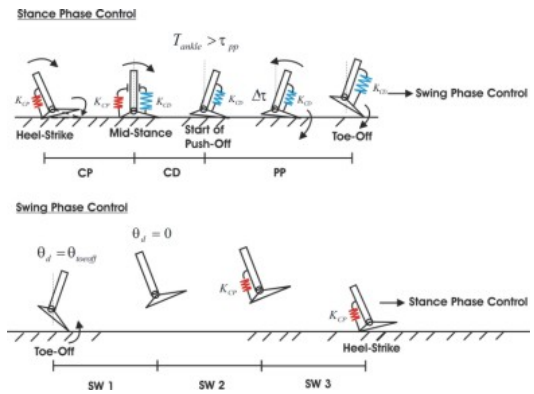

Fig. 8. The finite-state control for a typical gait cycle.

V. Sensors and Computing Platform

This section describes the electronics hardware used for implementing the proposed controller onto the MIT powered ankle-foot prosthesis. Fig. 9 shows the schematics of the overall computer system. The computer system contained an onboard computer (PC104) with a data acquisition card, power supply, and motor amplifiers. The system was powered by a 48V, 4000mAh Li-Polymer battery pack. A custom breakout board interfaced the sensors to the D/A board on the PC104 as well as provided power the signal conditioning boards. The system runs the Matlab Kernel for xPC target application. The target PC (PC104) can communicate with a host computer via Ethernet. The host computer sends control commands and obtains sensory data from the target PC104.

Three state variables, including heel/toe contact, ankle angle, and joint torque, were measured to implement the proposed finite-state controller. We installed a 5 kΩ linear potentiometer across the series springs to estimate the joint torque. We also mounted a 500-line quadrature encoder in between the parent link and child link mounting plates to measure the joint angle. Six capacitive force transducers were placed on the bottom of the foot: two sensors beneath the heel and four beneath the forefoot region.

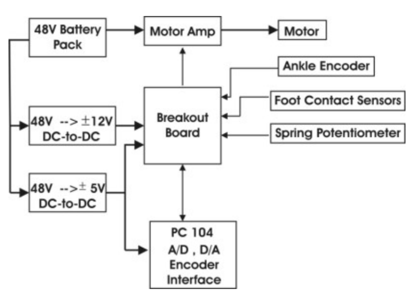

Fig. 9. Schematics of the overall computer system.

A mobile computing platform was developed that allowed us to conduct untethered walking experiments outside the laboratory. The mobile platform was mounted on an external frame backpack and most of the electronic components were mounted on the platform, including a PC104, a power supply, I/O Cards, and a motor amplifier. Using cabling, the prosthesis was connected to the I/O board and motor amplifier on the platform.

VI. Experiments

In this investigation, we measured the rate of oxygen consumption of three male, unilateral transtibial amputees(Ages: 40-57 yrs, Height: 173-176 cm, Weight: 71-86kg) walking at self-selected speeds for two conditions: (1) using their conventional passive prostheses; and (2) using the powered prosthesis. Their prostheses (with shoes) weighted about 1.5-2 kg, while the powered prosthesis weighted 3-4 kg, depending on the fitting of participants. Initial walking experiments were performed on the Johnson Indoor Track at MIT. Before conducting the metabolic cost study, each participant was given enough time to acclimatize to the powered prosthesis. Each participant communicated desired parameter values to a separate operator during the walking trails. By the end of the acclimatization, we obtained a set of control system parameters that provided the most favorable prosthetic ankle response at a self-selected walking speed.

We then measured the rate of oxygen consumption of the participant for the two experimental conditions. During the experiment, walking speed was controlled by having the participant follow a modified golf caddy set to a desired speed. The self-selected walking speed with the powered prosthesis was used for the two conditions. Sensory data (e.g. joint torque) from the prosthesis was also captured. Detailed information of the experimental protocol can be obtained from [16].

VII. Results and Discussion

During the experiments, it was discovered that the proposed finite state machine performed robustly and was capable of mimicking the target stance phase behavior. All amputee participants and the prosthetist were satisfied with the performance of the prosthesis. In general, it took less than 20 minutes for each amputee participant to adapt to the powered prosthesis. The prosthetist reported that with the powered prosthesis each participant moved with a more natural gait than with their conventional passive-elastic prosthesis.

Fig. 10 shows an experimental ankle torque-angle plot for one gait cycle. The experimental result demonstrates the system's capacity to track the target stance phase behavior and deliver sufficient net positive work at the ankle joint to propel an amputee. It is noted that the measured ankle torque-angle curve flattens around the peak torque region because the actual system took time (about 50ms) to output the offset torque. Also, the toe-off was set to be triggered before the ankle joint reaches the zero torque level (Fig. 10) because that can provide enough time for the control system to switch from impedance control mode to position control mode at the transition from stance to swing.

The measured, steady state rate to oxygen consumption

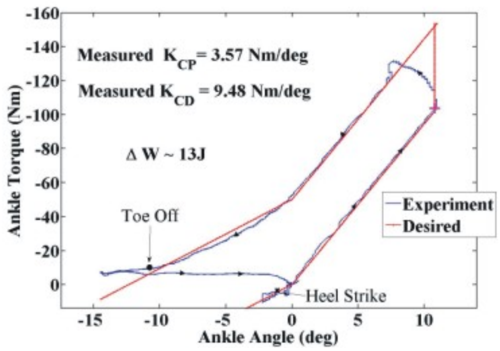

Fig. 10. An experimental ankle torque-angle plot for the powered prosthesis across a single gait cycle with positive net work. The red cross indicates the time at which the prosthesis begins actively plantar flexing.

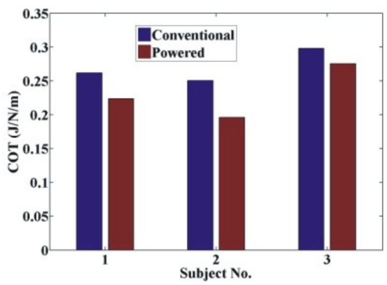

Fig. 11. The metabolic cost of transport for three participants.

was used to compute the metabolic cost of transport[2](COT), that is a standard measure of amputee walking economy. The standard formula from [19] was used to convert the rate of oxygen consumption into the metabolic power of walking. The metabolic COT for each participant is shown in Fig. 11. The powered prosthesis was found to decrease the COT of amputee participants from 7% to 20% compared to the conventional passive-elastic prostheses, even though the powered system was two-fold heavier than the conventional devices. This highlights the benefit of performing net positive work during stance to amputee ambulation. It also highlights the fact that the weight of the prosthesis is not necessarily a detriment to the clinical performance of a prosthetic intervention. Clearly, the weight of a powered ankle-foot prosthesis may not hinder an amputee's gait as long as the prosthesis can provide sufficient power output at terminal stance. In additional to the measurements, amputee participants reported that the powered prosthesis did not feel heavy when the system was active.

VIII. Conclusion

In this paper, a novel, powered ankle-foot prosthesis was built that comprises a unidirectional spring, configured in parallel with a force-controllable actuator with series elasticity. The prosthesis was controlled to mimic the normal human ankle walking behavior. The initial clinical study showed that the powered prosthesis improves amputee metabolic economy from 7% to 20% compared to the conventional passive-elastic prostheses, even though the powered system is twofold heavier than the conventional devices. These results highlighted the benefits of performing net positive work at the ankle joint to amputee ambulation. The future work includes developing a more viable prototype ankle-foot prosthesis that fits both human foot/ankle dimensions and geometry, with compact integrated battery and other electronic components. Also, it is necessary to conduct a comprehensive biomechanical gait study on the amputee participants to provide a biomechanical mechanism for the observed metabolic reduction. It is our hope that this work will lead to a new direction for further advancement of an ankle-foot prosthesis.

Acknowledgment

The authors wish to thank B. Deffenbaugh, and L. Magnusson for their contributions in the clinical study.

References

[1] D. A. Winter, "Biomechanical motor pattern in normal walking," *Journal of Motor Behavior*, Vol. 15, No. 4, pp. 302 - 330, 1983.
[2] M. Palmer, "Sagittal plane characterization of normal human ankle function across a range of walking gait speeds," *Master's Thesis,* Massachusetts Institute of Technology, 2002.
[3] D. H. Gates, "Characterizing ankle function during stair ascent, descent, and level walking for ankle prosthesis and orthosis design," *Master's thesis,* Boston University, 2004.
[4] S. Ron, *Prosthetics and Orthotics: Lower limb and Spinal.* Lippincott Williams & Wilkins, 2002.
[5] D. A. Winter and S. E. Sienko, "Biomechanics of below-knee amputee gait," *Journal of Biomechanics,* Vol. 21, No. 5, pp. 361-7, 1988.
[6] N. H. Molen, "Energy/speed relation of below-knee amputees walking on motor-driven treadmill," *Int. Z. Angew. Physio,* Vol. 31, pp.173, 1973.
[7] G. R. Colborne, S. Naumann, P. E. Longmuir, and D. Berbrayer, "Analysis of mechanical and metabolic factors in the gait of congenital below knee amputees," *Am. J. Phys. Med. Rehabil.,* Vol. 92, pp. 272 - 278, 1992.
[8] G. K. Klute, J. Czerniecki, and B. Hannaford, "Development of powered prosthetic lower limb,' *Proc. 1st National Mtg,* Veterans Affairs Rehab. R&D Service, Washington, DC, October 1998.
[9] S. H. Collins and A. D. Kuo, "Controlled energy storage and return prosthesis reduces metabolic cost of walking," *Proc. on ISB XXth Congress and the American Society of Biomechanics Annual Meeting,* Cleveland, Ohio, pp. 804, August 2003.
[10] C. Li, et al.,"Research and development of the intelligently-controlled prosthetic ankle joint," *Proc. of IEEE Int. Conf. on Mechatronics and Automation,* Luoyang, China, pp. 1114-1119, 2006.
[11] US Patent 6443993, Sept. 3, 2002.
[12] www.ossur.com.
[13] K. Koganezawa, and I. Kato, "Control aspects of artificial leg," *IFAC Control Aspects of Biomedical Engineering*, pp.71-85, 1987.
[14] S. K. Au, P. Dilworth, and H. Herr, "An ankle-foot emulator system for the study of human walking biomechanics," *Proc. IEEE Int. Conf. on Robotics and Automation,* Orlando, FL, pp. 2939-2945, May 2006.
[15] V. T. Inman, H. J. Ralston, and F. Todd, *Human walking.* Baltimore: Williams and Wilkins; 1981.
[16] S. K. Au, "Powered Ankle-Foot Prosthesis for the Improvement of Amputee Walking Economy," *Ph.D. Thesis,* Massachusetts Institute of Technology, 2007.
[17] D. Robinson, "Design and an analysis of series elasticity in closed-loop actuator force control," *Ph.D. Thesis,* Massachusetts Institute of Technology, 2000.
[18] D. L. Grimes, "An active multi-mode above-knee prosthesis controller," *Ph.D. Thesis,* Massachusetts Institute of Technology,1976.
[19] J.M. Brockway, "Derivation of formulae used to calculate energy expenditure in man," *Human Nutrition: Clinical Nutrition,* Vol. 41, pp. 463-471, 1987.

[2]The metabolic cost of transport is defined as the metabolic energy requires to move per unit distance per unit weight [15].